Theoretical Chemistry Accounts (2020) 139:80
https://doi.org/10.1007/s00214-020-02596-x

REGULAR ARTICLE

Quantum mechanics meets scaling theory near the critical point

Carlos Bistafa[1] · Tárcius N. Ramos[1] · Kaline Coutinho[1] · Sylvio Canuto[1]

Received: 25 January 2020 / Accepted: 25 March 2020 / Published online: 9 April 2020

Abstract
The critical point is believed to be not amenable to quantum mechanical calculations because the correlation length goes to infinity, the density is largely inhomogeneous and some thermodynamic properties diverge. For these reasons, until very recently all theoretical information of the critical point has been obtained by statistical physics and nothing was known about the electronic structure. Employing a sequential quantum mechanical/molecular mechanical (S-QM/MM) approach for a nonpolar atomic fluid, we study the behavior of the dielectric constant at different temperatures, ranging from dense fluid to supercritical condition. Our primary focus lies on the vicinity of the critical point. By using quantum mechanical calculations with thermodynamic condition, we perfectly reproduce the behavior found previously for classical monoatomic fluid by using scaling functions and renormalization theory that in the vicinity of the critical point the dielectric constant shares the critical behavior of the internal energy and, although the dielectric constant remains finite, its variation with temperature diverges. This perfect agreement leads credence to multiscale QM/MM methods and suggests the possibility of obtaining theoretical information about the electronic structure of a fluid near the critical point.

Keywords QM/MM · Critical point · Quantum chemistry · Electronic properties · Dielectric constant

1 Introduction

The critical point of a fluid is a singular point at the end of the coexistence line separating the gas and the liquid phases. At this point, the increasing density of the gas and the decreasing density of the liquid meet and this confluence point determines the boundary where supercritical fluid appears. As such, the critical point is characterized by very large fluctuations and density inhomogeneity. The behavior of different properties of the fluid at the critical point is the subject of great interest. It is well known, for instance, that the specific heat diverges at the critical point [1, 2]. Also it is known is that the density presents large inhomogeneity and equally important the correlation length goes to infinity. These aspects make one believe that the critical point is not amenable to quantum mechanical calculations. In fact, for several years all theoretical knowledge of the critical point was obtained by statistical physics [3]. Universal scaling functions [1, 4] and renormalization theory [4, 5] have been applied to understand the several aspects and the behavior of polar and nonpolar fluids undergoing transition to critical conditions. An important characteristic aspect of the critical point is that it is believed to be universal, thus not depending on the details of the system. The difficulty of assessing the critical point for quantum mechanical calculations imposes a severe limitation precluding the analysis of the electronic structure of a fluid near or at the critical point.

Using statistical physics, successful studies of the behavior of nonpolar fluids near the critical point were carried out. The behavior of the dielectric constant in the vicinities of the critical point has deserved considerable attention. Although the critical point is forbidden for quantum mechanical incursions, the vicinities may be accessible. An essential point in this endeavor is that QM alone is not sufficient and the specification of the thermodynamic condition is imperative to ascertain the precise location of the system in the phase diagram. A combination of QM with thermodynamic condition is possible using the multiscale QM/MM methodology. Using the sequential QM/MM (S-QM/MM) [6, 7], we have recently considered the case of Ar only 2 K above the critical

"Festschrift in honor of Prof. Fernando R. Ornellas" Guest Edited by Adélia Justino Aguiar Aquino, Antonio Gustavo Sampaio de Oliveira Filho & Francisco Bolivar Correto Machado.

✉ Sylvio Canuto
canuto@if.usp.br

[1] Instituto de Fisica, Universidade de Sao Paulo, Rua do Matão 1371, São Paulo, SP 05508-090, Brazil

temperature and obtained the dielectric constant value of 1.173 ± 0.005 [8], in excellent agreement with the experimental value of 1.179 [9]. In this same study [8], we pointed out for the first time that the dielectric constant shows a density-independent behavior around the critical density.

A few years ago, Bertrand et al. [10] used the complete scaling to study the critical behavior of a fluid in an electric field and found that the Clausius–Mossotti (CM) approximation can be obtained from thermodynamic theory in the mean-field regime. They suggested that, despite being only strictly correct in the mean-field approach, CM can still be useful for understanding the dielectric constant in the case of nonpolar fluids, since the error introduced is small. They [10] also argued that it would be very difficult to experimentally observe the singularity in the variation of the dielectric constant near the critical point. This is in line with previous theoretical results [11, 12] and with the absence of the experimental observations [13–15].

Naturally, while these studies take advantage of powerful statistical mechanical techniques that can even provide analytical solutions for cases where some approximations are adopted, none of them can describe the electronic structure of the system. Avoiding the critical point, but remaining in the close vicinity, it is in principle possible to combine QM and thermodynamic condition to obtain important information on the electronic structure, by using multiscale methods [16, 17], as QM/MM methods. The essential question at this point is whether quantum mechanics can prove its reliability by providing positive results in a crucial test.

A rather important study was made in a seminal work by Stell and Høye [11]. They used a theoretical analysis, based on the deviation of the CM equation for discussing properties of classical nonpolar fluids at the critical point. They found that: (1) the dielectric constant shares the critical behavior of the internal energy, (2) the dielectric constant ε is expected to be finite at the critical point (ε_c is finite), and (3) its derivative with respect to the temperature ($[\partial\varepsilon/\partial T]_c$) should diverge. These three points are non-trivial and were found using universal scaling laws on model systems (hard-sphere and Lennard-Jones fluid with constant atomic polarizability and variable polarizability depending on the position of the neighboring atoms) and are very challenging to be obtained by any other method. Sengers et al. [12] obtained a similar conclusion by employing universal scaling laws and renormalization-group theory for classical fluids. It is known that all fluids with short-range interactions, including polar fluids, are expected to belong to the same universality class [11, 12]. Therefore, the short-range interactions between the atoms in the fluid determine the nature of the critical point singularity. Experimental investigations reported finite values for ε_c although there are still some controversy about the behavior of the variation of ε ($\delta\varepsilon = \varepsilon - \varepsilon_c$) with respect to temperature variation ($t = T - T_c$) where apparently anomaly was not found for fluids [12–15]. In the experimental setup, the noxious volume effect could either create a spurious anomaly in ε or mask a true anomaly [12, 13].

The analysis of the three points of Stell and Høye [11] presented above, under the confines of quantum mechanics, is the challenge one considers in this work.

In the present study, we extend our previous QM/MM model [8], now discussing the dielectric constant dependence on the temperature, the comparison with the internal energy and its behavior near the critical point. As the critical point is believed to be universal, we conveniently selected the Ar fluid. The classical MM simulations are carried out using Metropolis Monte Carlo (MC) as explained in the next section as well as the QM that uses the density functional theory (DFT) quantum mechanical calculations.

As we will show our results agree with previously discussed theoretical works [10–12], which were performed using different statistical mechanical techniques, and show that with the current computational protocol QM/MM methods can, in principle, be used to study the electronic structure of atomic and molecular systems in the vicinities of the critical point.

2 Methods

We have employed the S-QM/MM [6, 7], where classical simulations are carried out first to generate configurations of the fluid in the desired thermodynamic condition. After the classical simulation is performed, all configurations are analyzed and only statically uncorrelated configurations are used to perform quantum mechanical calculations. This allows obtaining statistically convergent results with a relatively small number of configurations. This is of importance because these selected configurations will be used next in QM calculations, where the computational effort can be considerable. In this study, all the results presented are statistically stable and obtained from QM calculations on 200 configurations sampled from the MC simulation.

For sampling the configurations of the dense fluid argon, we carried out classical Monte Carlo Metropolis simulations in the *NPT* ensemble, by using the DICE code [18]. The calculations were performed on the isobaric line at 50 atm, which is higher, but close to the experimental critical pressure ($P_c = 48.18$ atm) [9]. The system used for the MC simulation was composed of 2500 argon atoms interacting by Lennard-Jones (LJ) potential, simulated in a cubic box with periodic boundary conditions and the image method. Standard procedure such as the sampling technique was described before [19]. The parameters used in the LJ potential were proposed by Maitland and Smith [20] ($\varepsilon_{LJ} = 0.2378$ kcal/mol and $\sigma_{LJ} = 3.41$ Å), which shows an accurate description

of thermodynamic properties near the critical point [8]. In addition, test calculations [8] of the specific heat c_v for Ar reproduced the experimental value for liquid condition ($T = 120$ K and density of 1.166 g/cm^3). After the system reaches the equilibrium, 2×10^9 MC steps were performed to calculate the average of density (ρ), internal energy per particle ($u = U/N$) and molar heat capacity (c_p). Fourteen temperature values between 130 and 180 K were used to perform the calculations of the dielectric constant. The reported experimental critical temperature is $T_c = 150.7$ K [9].

As discussed in our previous works [6–8], we used the autocorrelation function of the energy to select statistically uncorrelated configurations from the MC simulation (less than 10% of statistical correlation). For each temperature T, a total of 200 configurations were selected to be used in DFT quantum mechanical calculations of the static dipole polarizability. As we will see, this is enough to produce converged results in all cases. We employed the Kohn–Sham approach for the DFT calculations using the B3P86 exchange functional [21, 22] with the correlation consistent basis set [23] aug-cc-pVDZ. This is termed as B3P86/aug-cc-pVDZ. This calculation level has been selected because it was successfully used in our previous study [8], leading to very accurate results for the dielectric constant. The use of dispersion-corrected functionals has shown to be immaterial [8]. For each configuration i, we calculate the isotropic static dipole polarizability α_i of the central atom in the presence of the nearest 13 atoms, corresponding to the number of atoms present in the first solvation shell for the simulation at the dense fluid phase with 130 K and 50 atm. For consistency, we use this number of atoms for all cases. For each case, two calculations are needed: one with 14 atoms and another with 13 atoms (without the central atom) for obtaining the dipole polarizability of the central atom by subtraction. This is a valid approximation because the interacting contribution to the static polarizability is very small. This is one of the reasons for the general validity of the CM equation even for liquid or dense fluid phase in the case of Ar, as discussed before [24–26]. The use of the CM equation in our study deserves some observations. It relates the static dipole polarizability to the static dielectric constant for nonpolar gaseous systems. It is known to present limitations in the case of liquids because the overlap of the electron densities of the constituents should be considered. This is needed because in the liquid, or dense fluid, the atomic interaction should be considered. In the case of Ar, this correction is small, as discussed above. Note that in our QM calculations the atomic interaction is included naturally by considering the Schrödinger equation for the system, composed by all 14 atoms, sampled from the MC simulation. The Kohn–Sham determinant is antisymmetric over the entire system, and this allows the wave function delocalization over all atoms, thus including overlap naturally.

For each α_i, we obtained the dielectric constant ε_i, by using the CM equation:

$$\frac{\varepsilon_i - 1}{\varepsilon_i + 2} = \frac{4\pi}{3}\alpha_i \rho \frac{N_A}{M}, \quad i = 1, 2, \ldots, 200 \tag{1}$$

where ρ is the density of the system, N_A is the Avogadro constant and M is the molar mass. The final value of ε_i is presented as the average of 200 configurations at the same temperature. This procedure was performed for all the 14 temperature values considered, allowing us to discuss the behavior of the dielectric constant with the temperature. All DFT calculations were performed using the Gaussian 09 program [27]. In total, 5600 QM calculations at the B3P86/aug-cc-pVDZ level were performed in this study.

3 Results and discussion

First, we discuss the results obtained from the classical simulations. The calculated results for different properties including the molar heat capacity at constant pressure c_p are shown in Table 1.

The simulations were performed in fourteen different temperature values, ranging from the dense fluid to the

Table 1 Results obtained for different temperatures, from Monte Carlo simulation (density ρ, molar heat capacity at constant pressure c_p, module of internal energy per atom $|<U/N>|$) and from DFT calculations (dipole polarizability α, dielectric constant ε)

T (K)	ρ (g/cm^3)	c_p (kcal/mol K)	$\lvert<U/N>\rvert$ (kcal/mol)	$\alpha\left(a_0^3\right)$	ε (Dimensionless)
130	1.120	0.012	1.102	11.372	1.408
140	1.027	0.015	1.002	11.285	1.367
144	0.982	0.016	0.956	11.276	1.349
148	0.928	0.019	0.902	11.223	1.326
152	0.856	0.024	0.834	11.154	1.296
154	0.804	0.034	0.787	11.097	1.275
155	0.768	0.046	0.755	11.033	1.260
155.5	0.736	0.070	0.728	11.021	1.248
156	0.369	0.400	0.406	10.669	1.115
156.5	0.324	0.056	0.360	10.647	1.101
157	0.310	0.045	0.344	10.566	1.095
160	0.264	0.022	0.292	10.514	1.080
170	0.206	0.012	0.222	10.369	1.061
180	0.177	0.009	0.187	10.319	1.053

For the properties obtained in Monte Carlo simulation, the results are the average of all the sampled configurations (810,000); for the properties obtained by using DFT, the results are the average over 200 calculations, performed by using the selected configurations. The standard deviation is around ~ 6%, except for the thermodynamic properties at $T = 156$ K (the highest value of c_p), where the thermal fluctuation is higher (~ 20%)

supercritical phase, passing through the critical point region. The results for the molar heat capacity at constant pressure c_p are shown in Fig. 1. One can note the behavior of the molar heat capacity at constant pressure c_p suggesting the location of the critical temperature T_c near 156 K. The thermal conductivity also diverges at the critical point.

Additional evidence of the critical point can also be noted looking at the density. There is a discontinuity around 156 K (Fig. 2). Again, further calculations in the small interval close to 156 K are very difficult. Note that Fig. 2 indicates that the density remains finite at the critical temperatures, but its variation $\partial\rho/\partial T$ with the temperature diverges. For reference, we should mention that the experimental value of the critical density ρ_c is 0.531 g/cm^3.

We now analyze the radial distribution function $G(r)$ (Fig. 3). The continuous (blue) lines correspond to the dense fluid phase. As expected for a dense fluid, we can observe more than one solvation shell (related to the multiple peaks of the $G(r)$), indicating a well-structured dense fluid. This is in due agreement with experimental results [28]. At the fixed pressure of 50 atm, by increasing the temperature, the system eventually gets into the supercritical region. As the theoretical critical temperature T_c is found around 156 K, this is the transition point. And this is noted in Fig. 3 where the radial distribution functions within the supercritical region are represented by dotted (red) lines. Now the second peak becomes wider and decreases. This characterizes the supercritical region.

Let us now analyze the QM calculations that are the major focus of this study. As said before for each simulation at a given temperature, we selected 200 representative configurations, which were used for calculating the dipole polarizability using DFT B3P86/aug-cc-pDVZ calculations and, using these in the CM equation (Eq. 1), obtaining the dielectric constant. The result for each temperature was obtained as the average of the 200 configurations. The results are also

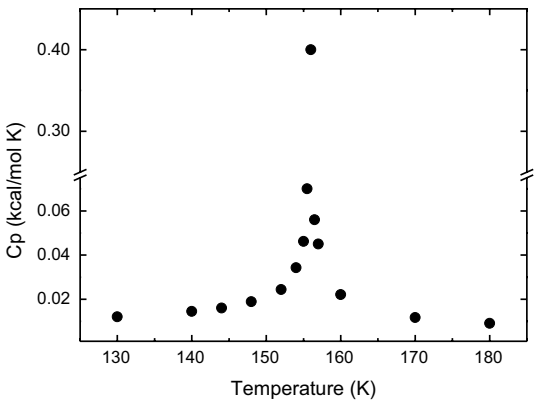

Fig. 1 Behavior of the molar heat capacity at constant pressure (50 atm) depending on the temperature. Note the evidence of divergence at $T \sim 156$ K

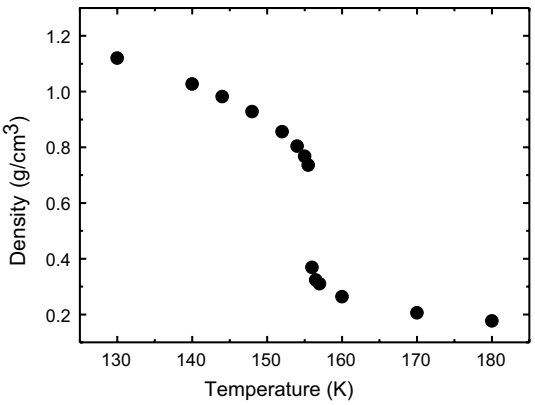

Fig. 2 Density of argon in several temperatures obtained from Monte Carlo simulations. There is a discontinuity around 156 K, indicating the critical temperature and the transition between dense fluid and supercritical phases

presented in Table 1. Each value of α presented in this table is the average of 200 QM α_i calculations. Now we examine the dielectric constant. For each temperature, the 200 values of α_i generate the equivalent 200 values of ε_i using the CM equation (Eq. 1). From this set of ε_i values, the average ε for the given fixed temperature was calculated. To show the convergence of the results, Fig. 4 shows the calculated average for one specific case. (We have selected $T = 155$ K and $P = 50$ atm.) Clearly, the distribution of calculated values of ε_i leads to a converged value for the dielectric constant, in this case $\varepsilon = 1.260$.

Finally, Fig. 5 shows the behavior of the dielectric constant with respect to the temperature varying from 130 to 180 K. The behavior of the dielectric constant depending on

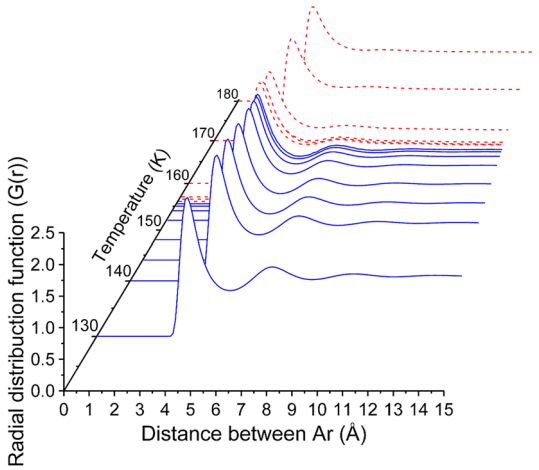

Fig. 3 Radial distribution function $G(r)$ of argon in different temperatures. Continuous (blue) lines correspond to the dense fluid phase, while dashed (red) lines indicate the supercritical phase. Note that in the supercritical phase, the fluid is less structured, with the $G(r)$ presenting just one solvation shell

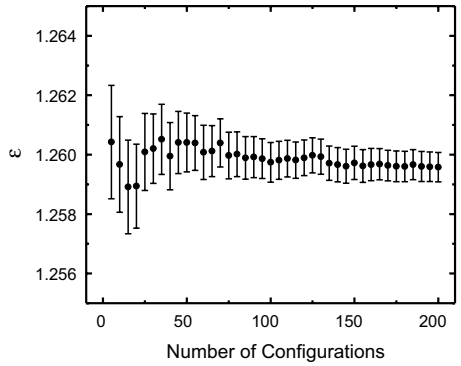

Fig. 4 Illustration of the statistical convergence of the calculated dielectric constant for one specific case $T = 155$ K. Converged values are ensured for all temperature value

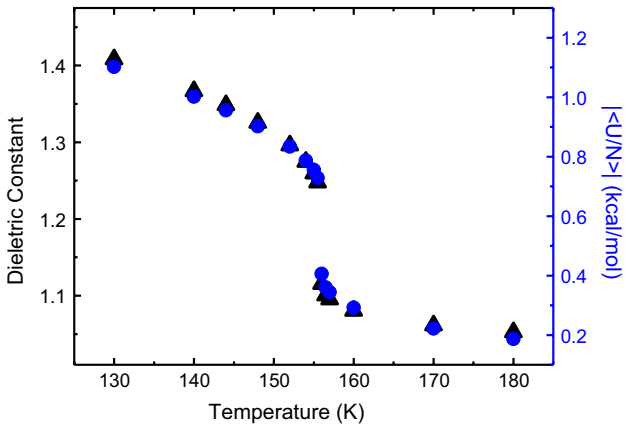

Fig. 5 Behavior of dielectric constant (black triangles) and internal energy (blue circles) with the temperature

the temperature is very clear: As the temperature increases, ε decreases. In spite of the fact that we cannot perform calculations at the critical point, we can clearly infer the result close to the critical point when it crosses the critical temperature T_c. We see in Fig. 5 that in the vicinity of the critical point, ε behaves as a well-defined, finite, quantity. However, there is an abrupt change between 155.5 and 156 K when the dielectric constant value rapidly decreases from 1.248 to 1.115 (Table 1). From the curve $\varepsilon(T)$, we see that $\partial\varepsilon/\partial T$ becomes infinity. Hence, we see an agreement with the studies of Stell and Høye [11] in that "*while the dielectric constant ε is expected to be finite at the critical point, its derivative with respect to the temperature should diverge*." There is an additional topic to analyze because Stell and Høye [11] also stated that the dielectric constant should share the behavior of the internal energy per particle. Thus, Fig. 5 also shows the internal energy per particle obtained from the Monte Carlo simulations, in an appropriate scale, and one can see a remarkable agreement. The absolute value of internal energy from the classical simulation follows the same behavior of the dielectric constant obtained from the QM calculations. At this point, one can see a perfect agreement between the results obtained by quantum mechanics and statistical physics using universal scaling laws. This is a most relevant theoretical aspect in spite of the possibility that effects derived from this behavior of the dielectric constant are possibly too small to be detected [10, 12].

4 Conclusions

We have studied the behavior of the dielectric constant of a nonpolar fluid (argon) in the vicinity of the critical point on an isobaric line. By using the S-QM/MM methodology, with different thermodynamic conditions, we have found at the critical point that the dielectric constant ε_c is finite, while $[\partial\varepsilon/\partial T]_c$ diverges. This is in remarkable agreement with finding from statistical physics methods using universal scaling laws. Also, we found that the dielectric constant follows the behavior of the internal energy per particle. Note that whereas the first property is obtained by quantum mechanical calculations, the second is obtained from the classical simulations. The classical simulations are used to provide the configurations for the quantum mechanical calculations. Thus, this clearly emphasizes the consistency of the results obtained here. Our quantum mechanical results not only agree with previous studies using scaling theory but also validate this outcome obtained before only for model systems. Extending the availability of theoretical methodologies used to describe and understand the properties of fluids in the critical region presents a possibility to study quantum mechanical properties of atoms/molecules in the close vicinity of such region. The possibility of explicitly include the thermodynamic condition in quantum mechanical calculations, or combining classical statistical mechanics and first-principles quantum mechanics may open large avenues for the study of atomic and molecular fluids and optimistically will permit to access the electronic properties of systems close to the critical point.

Acknowledgements The authors thank CAPES for the BioMol project 23038.004630/2014-35; the National Institute of Science and Technology of Complex Fluids (INCT-FCx) with the CNPq Grant 141260/2017-3 and FAPESP Grant 2014/50983-3; TNR thanks a FAPESP Grant 2015/14189-3. KC and SC acknowledge CNPq for continuous support. This work is dedicated to Prof. Fernando R. Ornellas on the occasion of his 70th birthday.

References

1. Fisher ME (1967) Rep Prog Phys 30:615–730
2. Fisher ME (1982) In: Hahne FJW (ed) Critical phenomena. Lecture notes in physics, vol 186. Springer, Berlin, pp 1–139

3. Domb C, Green MS (eds) (1972–1976) Phase transitions and critical phenomena, vol 1–6. Academic Press, London
4. Stanley HE (1999) Rev Mod Phys 71:S358–S366
5. Goldenfeld N (1992) Lectures on phase transitions and the renormalization group. Addison-Wesley, Boston
6. Coutinho K, Canuto S (2000) J Chem Phys 113:9132–9139
7. Coutinho K, Rivelino R, Georg HC, Canuto S (2008) In: Canuto S (ed) Solvation effects on molecules and biomolecules. Computational methods and applications. Springer, Berlin, pp 159–189
8. Hidalgo M, Coutinho K, Canuto S (2015) Phys Rev E 91:032115
9. Teague RK, Pings CJ (1968) J Chem Phys 48:4973
10. Bertrand CE, Sengers JV, Anisimov MA (2011) J Phys Chem B 115:14000–14007
11. Stell G, Høye JS (1974) Phys Rev Lett 33:1268–1271
12. Sengers JV, Bedeaux D, Mazur P, Greer SC (1980) Phys A Stat Mech Appl 104:573–594
13. Doiron T, Meyer H (1978) Phys Rev B 17:2141–2146
14. Chan MHW (1980) Phys Rev B 21:1187–1193
15. Thijsse BJ (1981) J Chem Phys 74:4678–4692
16. Warshel A, Levitt M (1976) J Mol Biol 103:227–249
17. Field MJ, Bash PA, Karplus M (1990) J Comput Chem 11:700–733
18. Coutinho K, Canuto S (2010) DICE, a Monte Carlo program for molecular liquid simulation, version 2.9. University of São Paulo, São Paulo
19. Cezar HM, Canuto S, Coutinho K (2019) Int J Quantum Chem 119:e25688
20. Maitland GC, Smith EB (1971) Mol Phys 22:861–868
21. Becke A (1993) J Chem Phys 98:5648–5652
22. Perdew JP (1986) Phys Rev B 33:8822–8824
23. Dunning TH (1989) J Chem Phys 90:1007–1023
24. Johnston DR, Oudemans GJ, Cole RH (1960) J Chem Phys 33:1310–1317
25. Amey RL, Cole RH (1964) J Chem Phys 40:146–148
26. Larsen SY, Mountain RD, Zwanzig R (1965) J Chem Phys 42:2187–2190
27. Frisch MJ, Trucks GW, Schlegel HB, Scuseria GE, Robb MA, Cheeseman JR, Scalmani G, Barone V, Mennucci B, Petersson GA, Nakatsuji H, Caricato M, Li X, Hratchian HP, Izmaylov AF, Bloino J, Zheng G, Sonnenberg JL, Hada M, Ehara M, Toyota K, Fukuda R, Hasegawa J, Ishida M, Nakajima T, Honda Y, Kitao O, Nakai H, Vreven T, Montgomery JA Jr, Peralta JE, Ogliaro F, Bearpark M, Heyd JJ, Brothers E, Kudin KN, Staroverov VN, Kobayashi R, Normand J, Raghavachari K, Rendell A, Burant JC, Iyengar SS, Tomasi J, Cossi M, Rega N, Millam JM, Klene M, Knox JE, Cross JB, Bakken V, Adamo C, Jaramillo J, Gomperts R, Stratmann RE, Yazyev O, Austin AJ, Cammi R, Pomelli C, Ochterski JW, Martin RL, Morokuma K, Zakrzewski VG, Voth GA, Salvador P, Dannenberg JJ, Dapprich S, Daniels AD, Farkas O, Foresman JB, Ortiz JV, Cioslowski J, Fox DJ, (2009) Gaussian 09 Revision D.01. Gaussian Inc, Wallingford, CT
28. Mikolaj PG, Pings CJ (1967) J Chem Phys 46:1401–1411